Electronic supplementary information (ESI)

A rare alb-4,8-Cmce metal-coordination network based on tetrazolate and phosphonate functionalized 1,3,5,7-tetraphenyladamantane

Ishtvan Boldog,[a] Konstantin V. Domasevitch,*[b] Igor A. Baburin,*[c] Holger Ott,[d] Beatriz Gil-Hernández,[e] Joaquín Sanchiz,*[e] Christoph Janiak*[a]

[a] Institut für Anorganische Chemie und Strukturchemie, Universität Düsseldorf, Universitätsstr. 1, D-40225 Düsseldorf, Germany. Email: janiak@uni-duesseldorf.de
(Ishtvan Boldog, Email: ishtvan.boldog@gmail.com)

[b] Inorganic Chemistry Department, Taras Schevchenko National University of Kiev, Volodymyrska Street 64, Kyiv 01033, Ukraine. Email: dk@univ.kiev.ua

[c] Institut für Physikalische Chemie und Elektrochemie, Technische Universität Dresden, Mommsenstr. 13, D-01062 Dresden, Germany. Email: igor.baburin@chemie.tu-dresden.de

[d] Holger Ott, Bruker AXS GmbH, Östliche Rheinbrückenstraße 49, Karlsruhe, D-76187, Germany. Email: Holger.Ott@bruker-axs.de

[e] Departamento de Química Inorgánica, Universidad de La Laguna, c/o Astrofísico Francísco Sánchez s/n, 38206 La Laguna, Spain. E-mail: jsanchiz@ull.es
(B. Gil-Hernández, Email: beagher@ull.es)

Content

General information

Single crystal X-ray diffraction experiments were performed on a Bruker APEX II QUAZAR system equipped with a multilayer mirror and an IμS molybdenum Kα source (λ = 0.71073 Å). The powder X-ray diffraction (PXRD) measurements were performed on a finely ground sample which was equally distributed on a low background silicon sample holder. The diffractograms were recorded with a Bruker D2 PHASER with Lynxeye 1D detector and Ni-filtered copper Kα radiation (30kV, 10mA generator parameters; restricted by a 0.6 mm divergence slit and a 1° Soller collimator) with a 0.02° step width. The simulated PXRD patterns were generated using Mercury 2.3 [1], with 0.02° steps and a FWHM(2θ) = 0.1°. A scaling with an adapting exponential function was used to achieve a better fit with the experimental data. ^{1}H and ^{13}C spectra were recorded on a Bruker Avance DRX-200 and a Bruker Avance DRX-500 spectrometer, respectively. FT-IR spectra were recorded using a Bruker Tensor 37 system equipped with an ATR unit (Platinum ATR-QL, Diamond) in the 4000-550 cm^{-1} region with 2 cm^{-1} resolution. Melting point determinations were performed in an open capillary using a Büchi-B450 apparatus. Sorption measurements were done using a Quantachrome iQ MP automatic gas sorption analyzer. The thermogravimetric (TG-DTA) analyses of $H_4L^1 \cdot 6.5H_2O$ and **1** were performed on a Netzsch STA 449 C Jupiter instrument coupled with a Pfeiffer Thermostar GSD 300 mass spectrometer at 10°C/min heating rate in air using corundum sample holders. Alternatively, the TG data for **2** were collected using a Netzsch Tarsus 209 F3 TGA instrument in a protecting flow of nitrogen (10 ml / min) at 5°C/min heating rate.

Magnetic susceptibility measurements on polycrystalline samples were carried out in the temperature range 1.9–300 K by means of a Quantum Design SQUID magnetometer operating at 10000 Oe. Diamagnetic corrections of the constituent atoms were estimated from Pascal's constants. Experimental susceptibilities were also corrected for the magnetization of the sample holder.

Syntheses

Synthesis of 1,3,5,7-tetrakis(4-cyanophenyl)adamantane, Ad(PhCN)$_4$

A mixture of 47.2 g (50 mmol) of 1,3,5,7-tetrakis(4-iodophenyl)adamantane [2], 21.5 g (240 mmol) of copper cyanide in 470 ml of anhydrous DMF distilled over CaH_2 were mildly refluxed with stirring in a 1L round bottom flask under argon for 7h. The formed copper iodide precipitate was removed by filtration after cooling the contents of the flask to r.t. The filtrate was concentrated to 200 ml under reduced pressure and poured while hot in 600 ml of water containing 30 ml of ethylenediamine. The resulting precipitate was separated by filtration and washed by copious amount of water. It was re-dissolved in 200 ml of hot DMF and while hot poured in 600 ml of 10% HCl. The precipitate was separated as described above, dried on air, dissolved in 100 ml of hot DMF and precipitated by addition of 100 ml of iPrOH. After cooling the mother liquor in the fridge (~4°C), the resulted precipitate was collected by filtration and dried at 80°C to give 22.17 g (82%) of the product as a white powder.

^{1}H NMR (DMSO-d_6, 500 MHz): δ= 2.12 (s, 12H); 7.80 (broad s, 16H). ^{13}C NMR (DMSO-d_6, 500 MHz): δ= 44.5 (**C**$_{Ad}$H$_2$), 109, 119, 127 (**C**$_{Ar}$H), 132 (C$_{Ar}$H), 154. m.p. (in open capillary): 385°-398°C with oxidation / decomposition.

FT-IR (neat) ν, cm^{-1}: 3500-2900 (w, br), 2928 (w, sh), 2854 (w), 1645 (vs), 1496 (w), 1450 (m), 1418 (m), 1384(s, sh), 1253 (w), 1105 (m), 1060 (w), 1008 (m), 841 (m), 788 (w), 761 (s), 729(w), 678 (m), 662 (m).

Synthesis of 1,3,5,7-tetrakis(4-phenyltetrazol-5-yl)adamantane hydrate, $H_4L^1 \cdot 6.5H_2O$

A mixture of Ad(PhCN)$_4$ (7.03 g, 13 mmol), sodium azide (8.45 g, 130 mmol) and anhydrous $ZnCl_2$ (10.61 g, 78 mmol) was mildly refluxed in 500 ml of DMF for 7 h under inert atmosphere and stirring. After cooling, the slightly yellow solution with minor amount of white precipitate was poured in 500 ml of cold (0°C) 10% HCl under stirring. The formed precipitate collected by filtration after 1h of staying, washed by 2x50 ml of 10% HCl solution and 3x50 ml of distilled water. The crude product containing DMF as a primary impurity was suspended in 300 ml of H_2O and concentrated ammonia was added drop-wise to the stirred slurry heated at 60°C until formation of a clear solution. It was acidified by addition of small portions of 5% HCl solution until a pH of 2 was achieved. The formed precipitate was collected by filtration after cooling to r.t., washed by 5x50 ml of distilled water and dried at 80°C until constant weight to afford 9.25g of white powder, which composition corresponds to $H_4L^1 \cdot 6.5H_2O$ hydrate.

^{1}H NMR (DMSO-d_6, 400 MHz): δ= 8.05 (d, 8H, J = 8.4 Hz), 7.89 (d, 8H, J = 8.4 Hz) , 2.250 (s, 12H). m.p. (in open capillary): no melting, gradual decomposition starts at >250°C (20 K/min heating rate). FT-IR (neat) ν, cm^{-1}: 3500-2400 (m, wb), 2933 (m), 2857 (m), 2740 (m), 1617 (s), 1565 (m), 1499 (s), 1434 (m), 1359 (m), 1247 (w), 1180 (w), 1155 (w), 1067 (m), 1025 (m), 996 (s), 896 (w),

840 (s), 785 (m), 751 (s), 727 (m), 703 (m), 574 (s). Elemental analysis, calcd (%) for $C_{38}H_{45}N_{16}O_{6.5}$ (829.88): C 55.00, H 5.47, N 27.01, found C 54.92, H 5.08, N 27.83%.

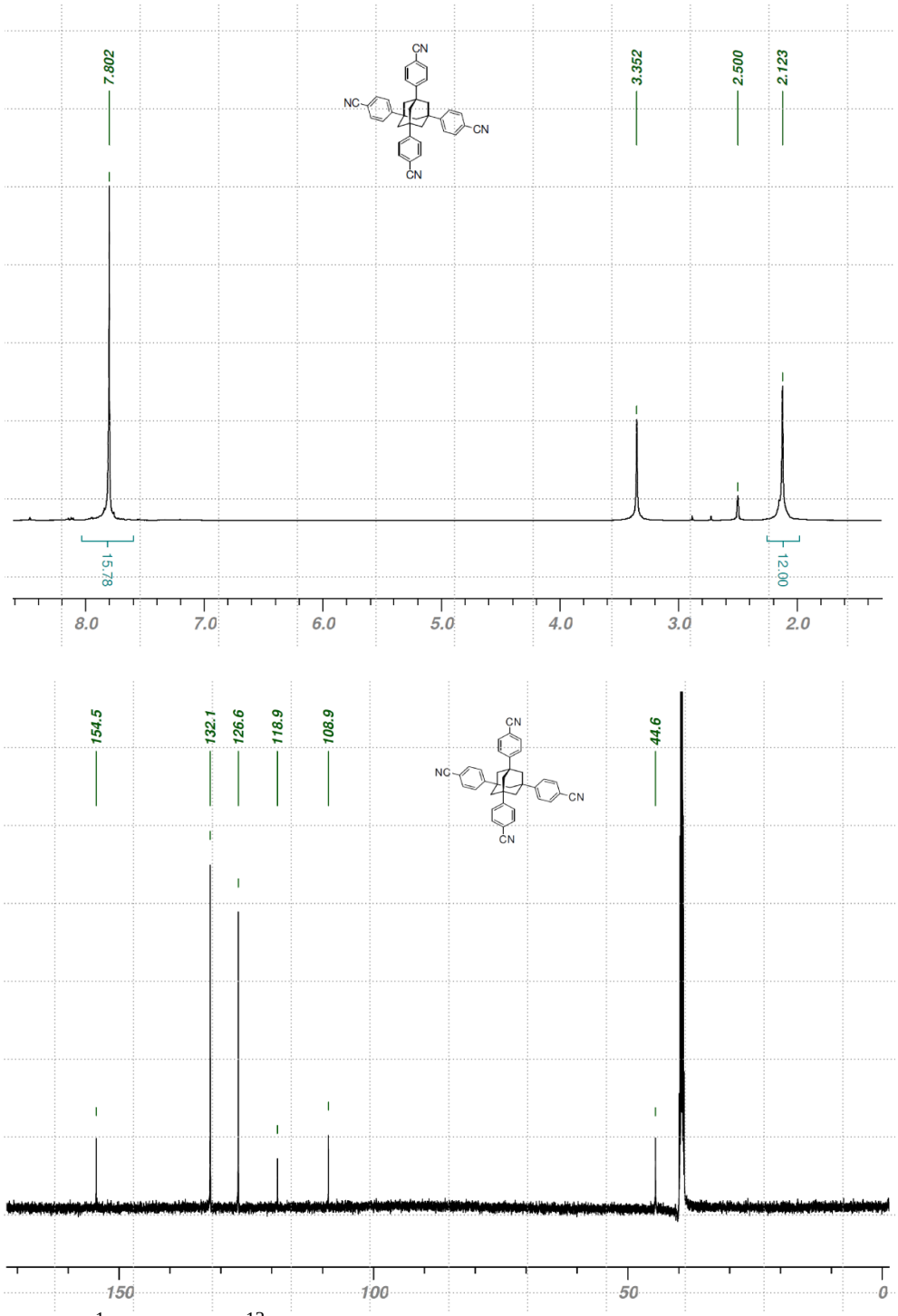

Fig. S1 ^{1}H (top) and ^{13}C (bottom) spectra of $Ad(PhCN)_4$ in DMSO-d_6.

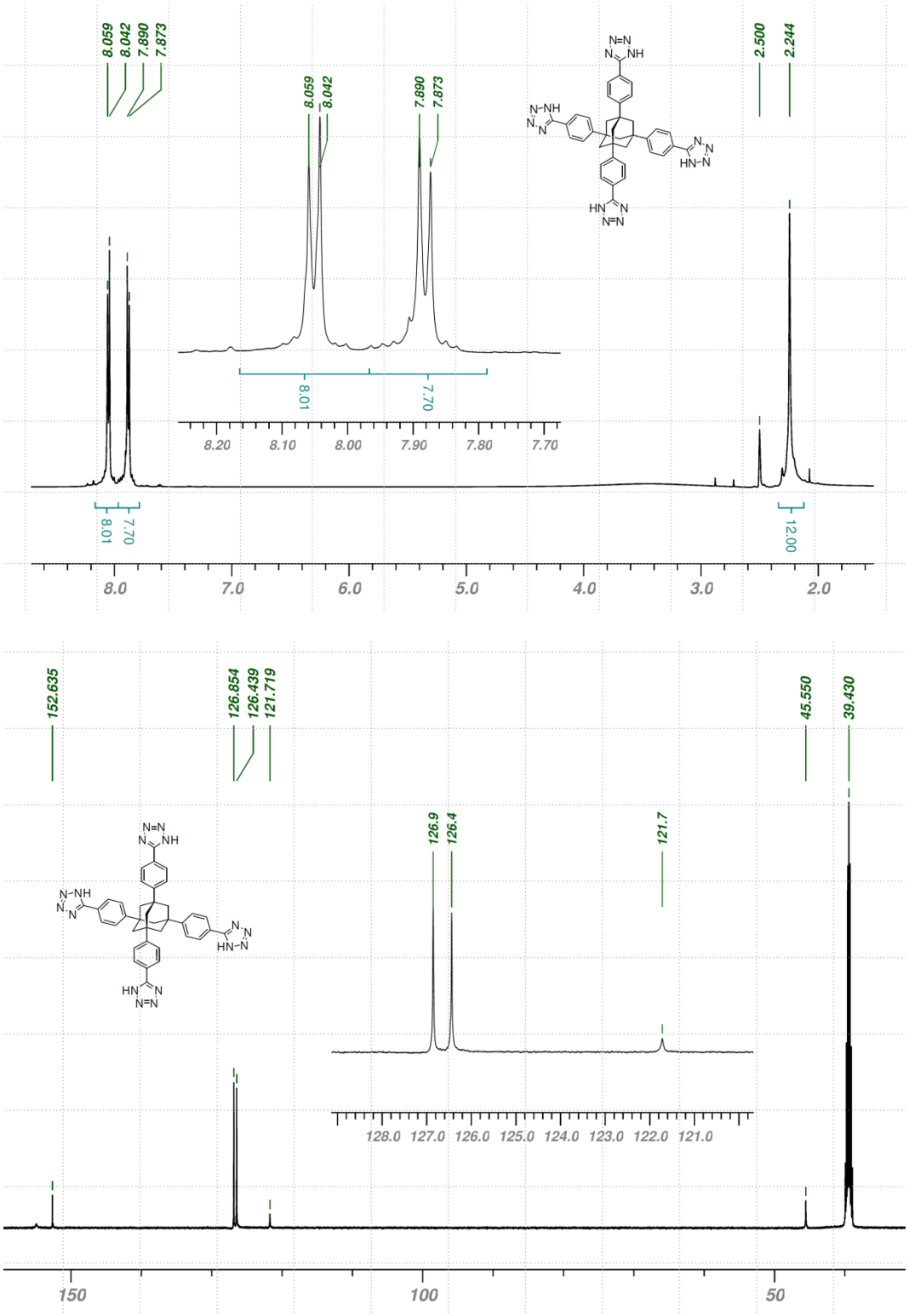

Fig. S2 ^{1}H (top) and ^{13}C (bottom) spectra of $H_4L^1 \cdot 6.5H_2O$ in DMSO-d_6.

Structural data and related information

Experimental details and crystal data for $[Mn_5Cl_2(L^1)_2(H_2O)_4(DMF)_4] \cdot x\ H_2O \cdot y\ DMF\ z\ H_2O$, ***1-as*** *(as synthesized)*

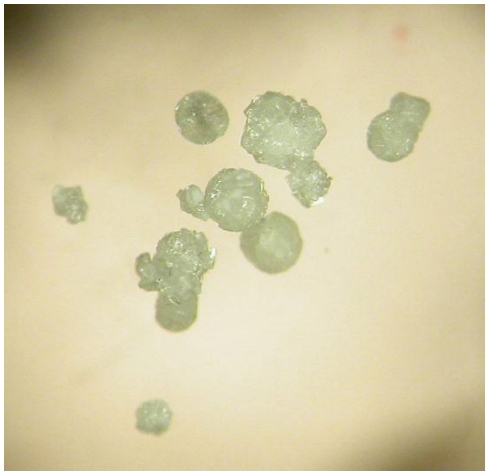

Fig. S3 The globular stellated co-grown crystals of **1-as** (as synthesized), as formed during the crystallization process

The crystals of **1-as** grew inherently as polycrystalline aggregates with some single-crystalline domains. All attempts to separate a single crystal from the bulk material were unsuccessful and a two component non-merohedral twin was measured. The indexing of the two twin domains was done using the Reciprocal Lattice Viewer tool in APEX2.[3] The data of the twin integration with SAINT 7.68a[4] were corrected for absorption with TWINABS 2008/4[5] and the de-twinned HKLF 4 file was used for the space group determination and structure solution with XS.[6] The structure refinement with XL6 is based on the HKLF 5 file, which contains reflections of the main component and all overlapping reflections with the second twin component.

All non-hydrogen atoms of the main (i.e. 'framework') residue were refined anisotropically, except for disordered guest and coordinated solvent molecules. According to the difference Fourier maps, the oxygen atoms O1 and O2 belong to site-sharing coordinated DMF (main component), water and MeOH [1] (minor components) molecules. In the second case, a two component DMF / water site-sharing model was partially refined, while in the first only the main DMF was refined. All residual electronic peaks with an absolute value exceeding 1.3 e / Å^3 were modeled as C or O atoms of guest solvent molecules.

[1] The composition of the material which was dried overnight in vacuo, with most of the MeOH molecules removed, was derived from the results of elemental analysis as $[Mn_5Cl_2(L^1)_2(H_2O)_4(DMF)_4] \cdot 3\ H_2O \cdot 7\ DMF$.

All the hydrogen atoms of C-H bonds were idealized and refined with bond length and isotropic displacement factor constrains.

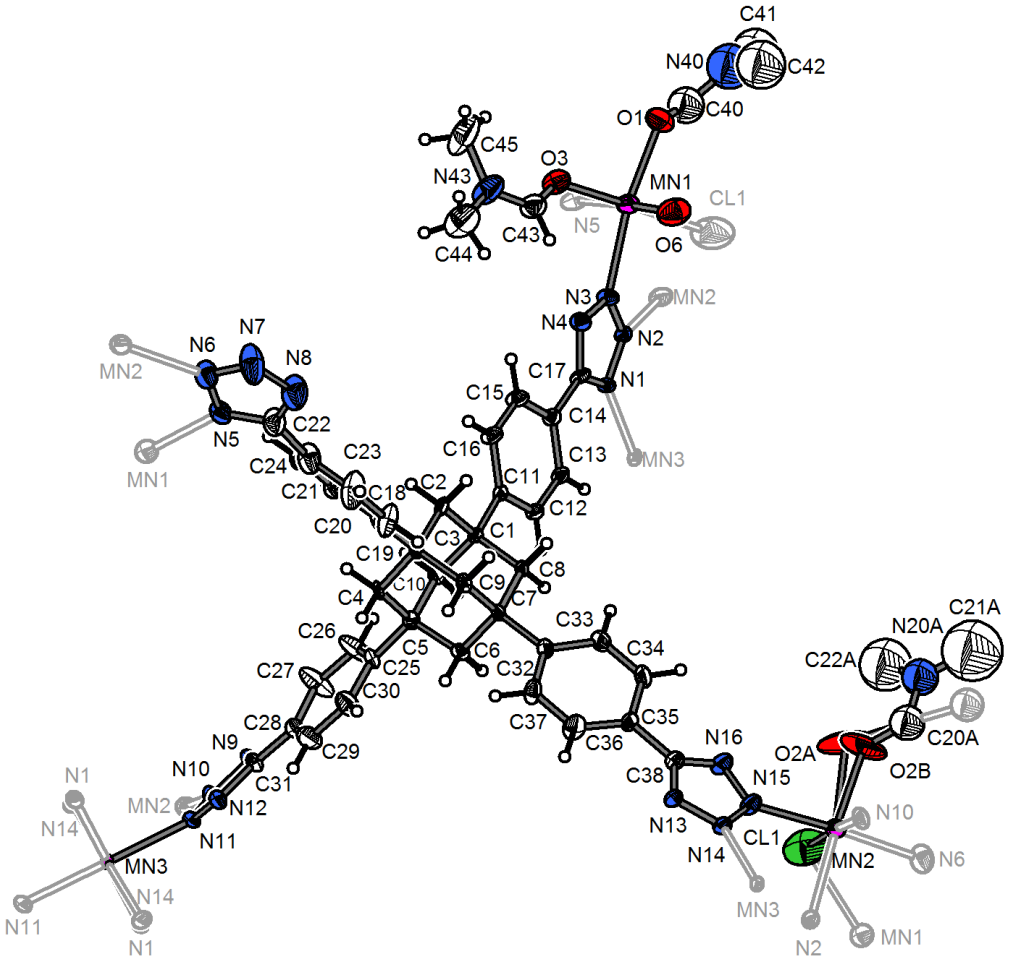

Fig. S4 ORTEP style representation (50% probability ellipsoids) of the asymmetric unit of $[Mn_5Cl_2(L^1)_2(H_2O)_4(DMF)_4] \cdot x\ H_2O \cdot y$ DMF z H_2O, **1-as** with atom numbering and the directly bound symmetry equivalent atoms (shown in gray without filling). The solvent molecules are not shown for clarity.

The answers on the crystallographic problems indicated by the IUCr's *checkCIF* service based on the Platon validation procedure (levels A and B) are given below:

Alert level A

PLAT222_ALERT_3_B Large Non-Solvent H Uiso(max)/Uiso(min) .. 10.0 Ratio

The atom in this alert belonsg to disordered molecules or site-sharing solvent molecules.

PLAT601_ALERT_2_A Structure Contains Solvent Accessible VOIDS of . 360 A**3

The structure is porous and not all guest molecules were modeled.

Alert level B

PLAT201_ALERT_2_B Isotropic non-H Atoms in Main Residue(s) 5

These atoms belong to a coordinated DMF molecule, which have a s.o.f. < 1 (the other component is water). In this case the non-coordinated atoms of the molecules with a partial occupancy were refined isotropically.

PLAT220_ALERT_2_B Large Non-Solvent C Ueq(max)/Ueq(min) ... 10.0 Ratio

PLAT220_ALERT_2_B Large Non-Solvent N Ueq(max)/Ueq(min) ... 7.7 Ratio

The two atoms in these alerts belong to disordered molecules or site-sharing solvent molecules.

PLAT306_ALERT_2_A Isolated Oxygen Atom (H-atoms Missing ?) O11

This is a water molecule and the hydrogen atoms were not refined according to the low quality of the data.

Experimental details and crystal data for $[La_2(H_2O)_6(H_5L^2)_2] \cdot Solv$, ***2***

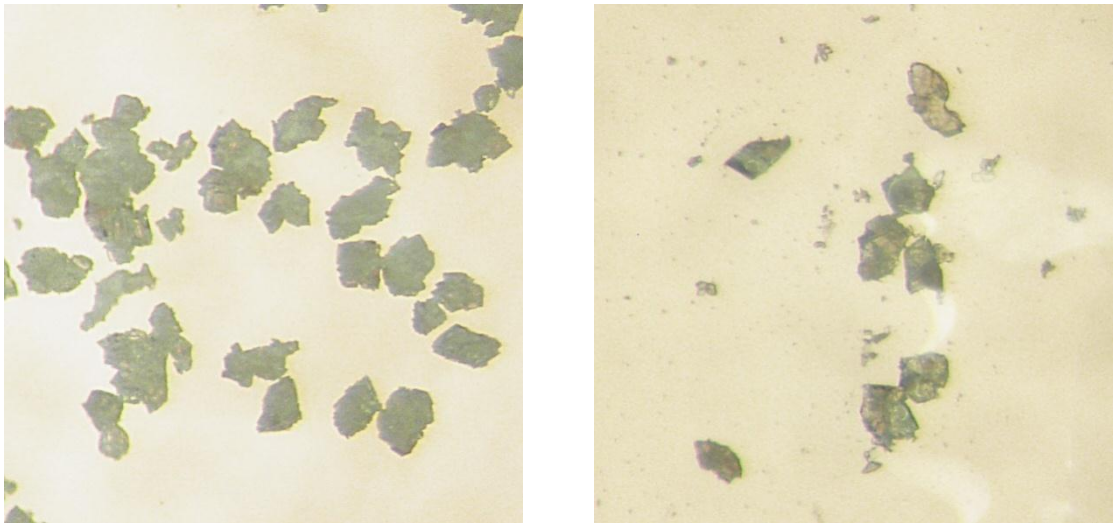

Fig. S5 Co-grown crystals of **2** after drying in air; the optical quality of the crystals remained satisfactory.

Small single crystals of **2** were found in the crystalline bulk material next to larger intergrown crystals (Fig. SS5). It was possible to perform the measurement on a tiny 0.03×0.07×0.08 mm single crystal, which was only diffracting to a resolution of 0.87 Å. The low diffracting power originates from the crystal size, guest molecules in the cavities and disorder in the crystal.

The structure was solved and refined by full-matrix least squares method using the SHELX-97 program package.6 All non-hydrogen atoms were refined using anisotropic displacement parameters including the guest molecules, i.e. water and MeOH. Due to diffuse packing of solvent molecules in combination with an average data resolution, not all solvent molecules could be located. SQUEEZE (PLATON) could be used to decrease the R1 (7.12 % in this case) but was not included for the reported structure as some of the guest molecules are participating in the hydrogen bonded network, which could be a matter of interest of a reader.

One of the phenyl groups (C1 – C6) was modeled as disordered over two positions, with the two components related through the C1 – C4 axis. The population factors were refined freely to give a 61/39 ratio.

All hydrogen atoms of the C-H bonds were idealized and refined with thermal displacement factors being of 1.2-fold or 1.5-fold (for the case of primary carbon atoms) of the 'parent' atoms' values. It was impossible to locate reliably the hydrogen atoms belonging to the phosphonic acid groups or most the guest molecules.

The answers on the crystallographic problems indicated by the IUCr's *checkCIF* service based on the Platon validation procedure (levels A and B) are given below:

Alert level A

PLAT601_ALERT_2_A Structure Contains Solvent Accessible VOIDS of . 383 A**3
Not all the guest molecules in the voids were modeled because of weak average intensities collected during the diffraction experiment from a very small crystal.

Alert level B

CHEMW03_ALERT_2_B WARNING: The ratio of given/expected molecular weight as calculated from the _atom_site* data lies outside the range 0.95 <> 1.05
PLAT043_ALERT_1_B Check Reported Molecular Weight 950.47
The molecular weight is given only for the main residue, which was defined to consist of molecules directly coordinated to the metal center (i.e. the guest molecules were not counted).

THETM01_ALERT_3_B The value of sine(theta_max)/wavelength is less than 0.575.
Calculated sin(theta_max)/wavelength = 0.5750
The relatively low resolution data is explained by weak diffraction at high angles from the available very small and porous crystal.

PLATPLAT430_ALERT_2_B Short Inter D...A Contact O1S .. O11 .. 2.67 Ang.
PLAT430_ALERT_2_B Short Inter D...A Contact O1S .. O9 .. 2.72 Ang.
PLAT430_ALERT_2_B Short Inter D...A Contact O4S .. O15 .. 2.75 Ang.
The listed values are not exceptional, but rather typical for charge assisted O-H···O bonds between phosphates/phosphonates and water.

Table S1 Crystal data and structure refinement for $[Mn_5Cl_2(L^1)_2(H_2O)_4(DMF)_4] \cdot x\ H_2O \cdot y$ DMF z H_2O, **1-as** and $[La_2(H_2O)_6(H_5L^2)_2] \cdot$ Solv, **2**

	1-as	**2**
Empirical formula	$C_{109}H_{147}Cl_2Mn_5N_{43}O_{18}$	$C_{34}H_{39}LaO_{15}P_4$
M_r /g mol^{-1}	2693.21	950.47
T /K	100(2)	120(2)
Wavelength / Å	0.71073	0.71073 Å
Crystal system	Monoclinic	Monoclinic
Space group	$P2_1/c$	C2/c
a /Å	17.4047(13)	22.6358(7)
b /Å	26.943(2)	19.0353(5)
c /Å	17.9892(15)	27.9879(11)
β /°	106.941(4)	110.636(2)
V /Å^3	8069.8(11) Å^3	11285.6(6)
Z	2	8
Calc. density / g cm^{-3}	1.108	1.119
μ / mm^{-1}	0.481	0.917
F(000)	2933	3840
Crystal size / mm^3	0.32 x 0.12 x 0.10	0.08 x 0.07 x 0.03
θ range /°	1.44 - 25.03	1.44 - 24.12
Index ranges / *hkl*	–20,19; 0,32; 0;21	–26,25; –21,21; –27,32
Reflections collected	14255	38944
Independent reflections	14255	8916 [R_{int} = 0.0771]
Completeness /% to theta /°	100 / 25.03	99.5 / 24.12
Absorption correction	Empirical	multi-scan
Max. and min. transmission	0.9535 and 0.8614	0.9730 and 0.9302
Refinement method	Full-matr. lst-sq. on F^2	Full-matr. lst-sq. on F^2
Data / restraints / parameters	14255 / 25 / 760	8916 / 51 / 600
Goodness-of-fit on F^2	1.092	1.051
Final R indices [I>2σ(I)]	R1 = 0.0954, wR2 = 0.2587	R1 = 0.0995, wR2 = 0.2592
R indices (all data)	R1 = 0.1153, wR2 = 0.2776	R1 = 0.1627, wR2 = 0.3014
Largest diff. peak and hole, e.Å^{-3}	1.168, –1.040	1.960, –0.954

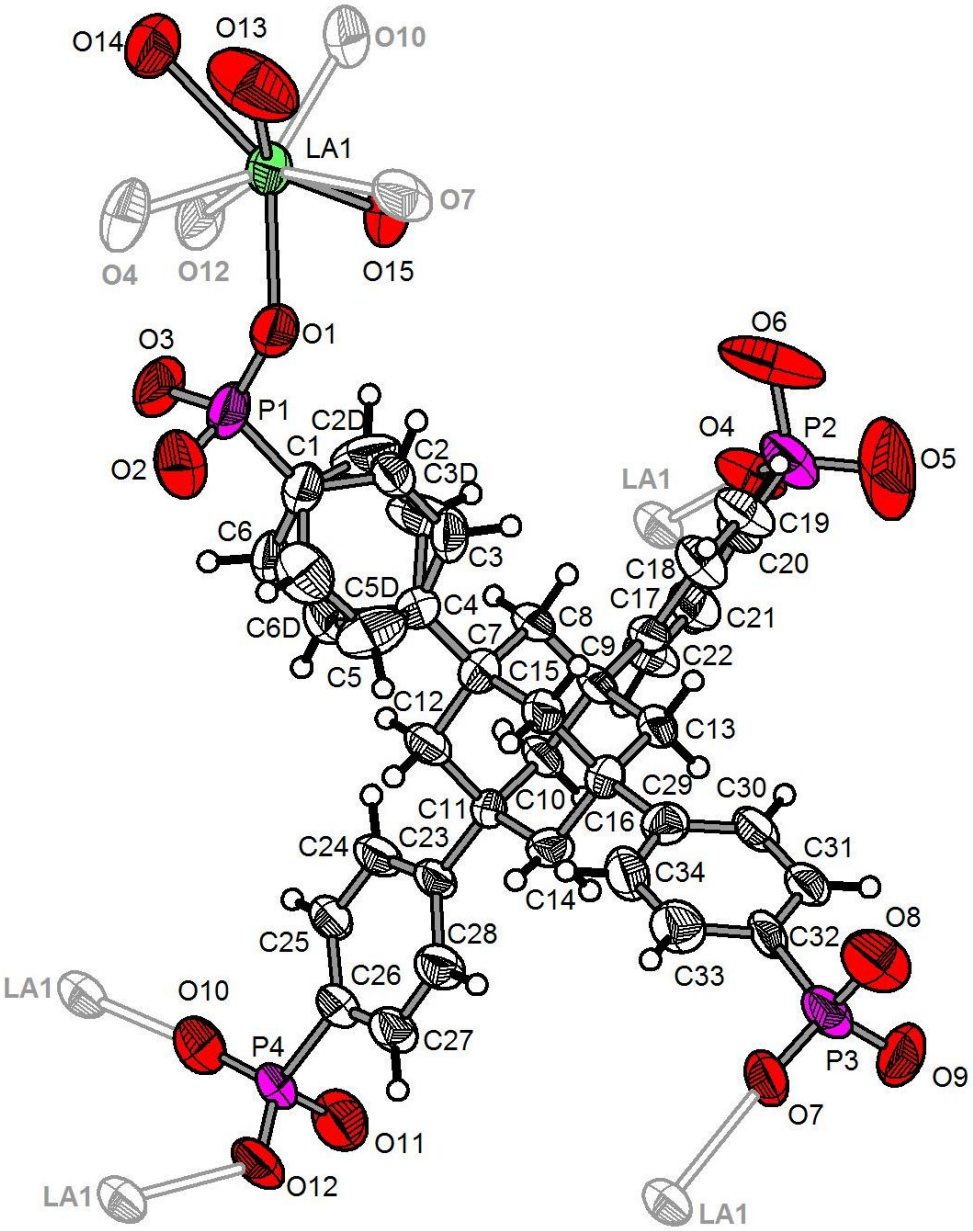

Fig. S6 ORTEP style representation (50% probability ellipsoids) of the asymmetric unit of $[La_2(H_2O)_6(H_5L^2)_2] \cdot Solv$, **2** with atom numbering and the directly bound symmetry equivalent atoms (shown in gray without filling). The solvent molecules are omitted for clarity.

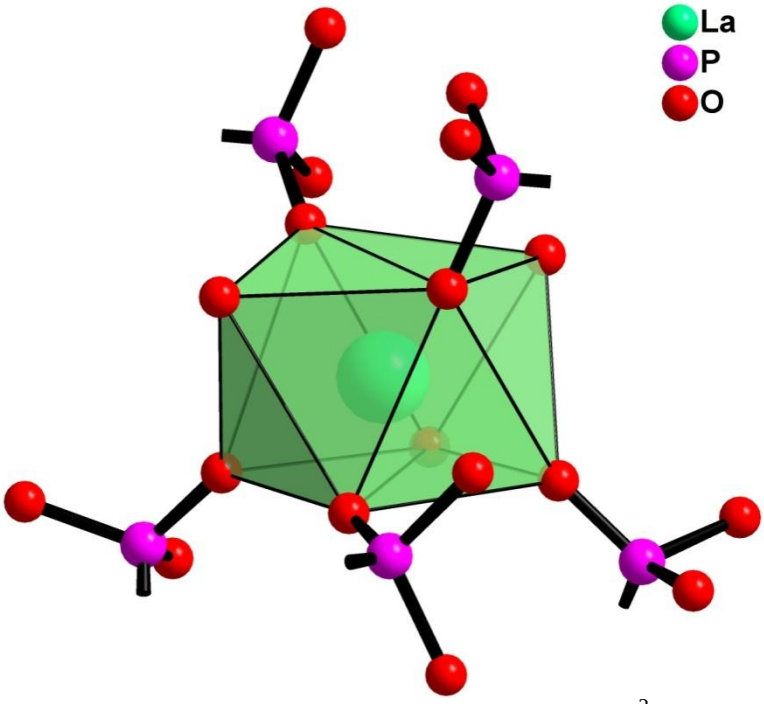

Fig. S7 The coordination environment of lanthanum in $[La_2(H_2O)_6(H_5L^2)_2]$, **2**, which is close to tetragonal-antiprismatic, with five oxygen atoms of phosphonate/phosphonic acid groups and three oxygen atoms of water molecules.

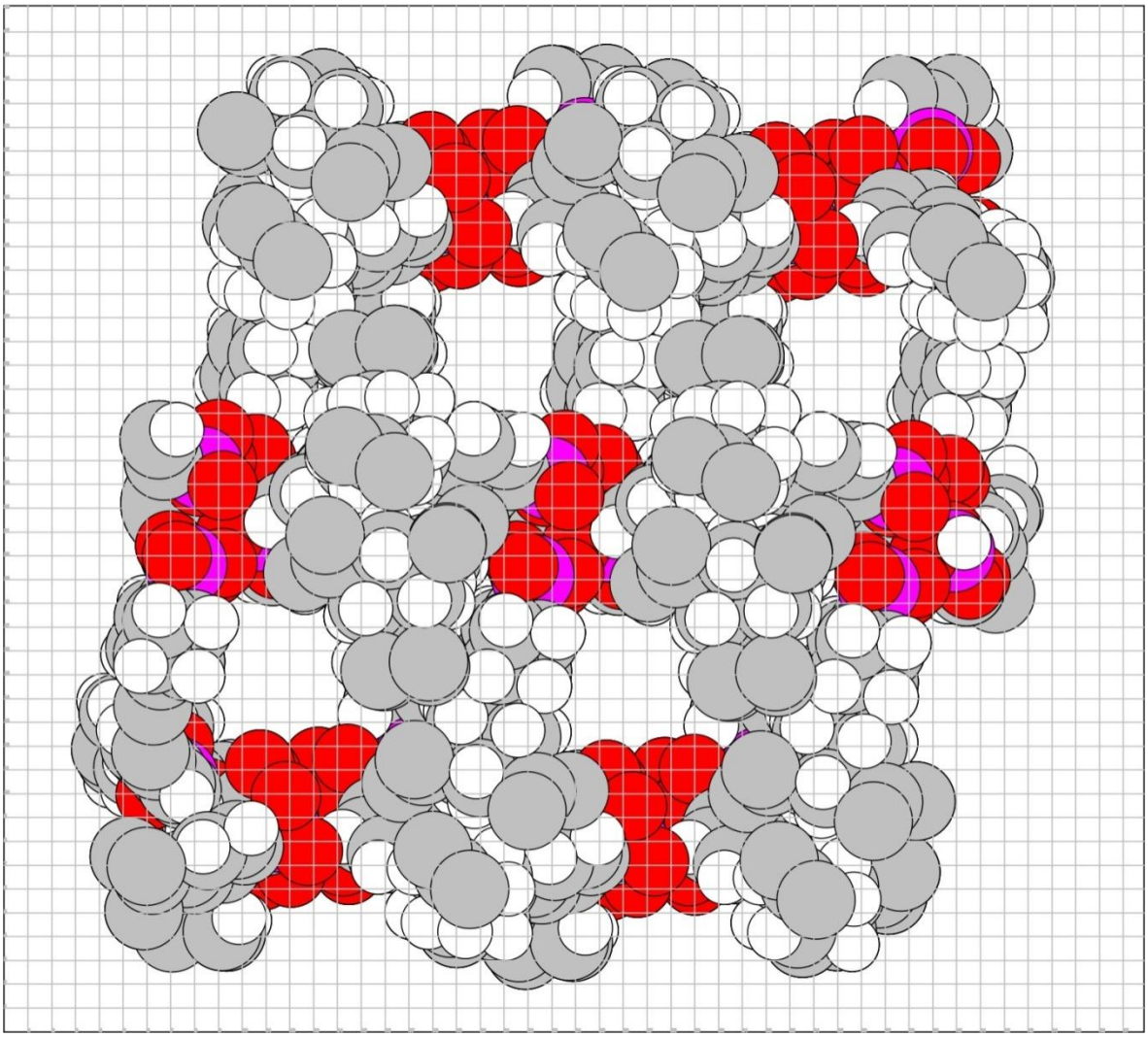

Fig. S8 A projection of space filling model of the $[La_2(H_2O)_6(H_5L^2)_2] \cdot$ Solv, **2** compound with a superimposed 1 Å grid to demonstrate the ~4 x 4 Å pores.

CSD based statistics of Mn-N bond length in tetrazolates

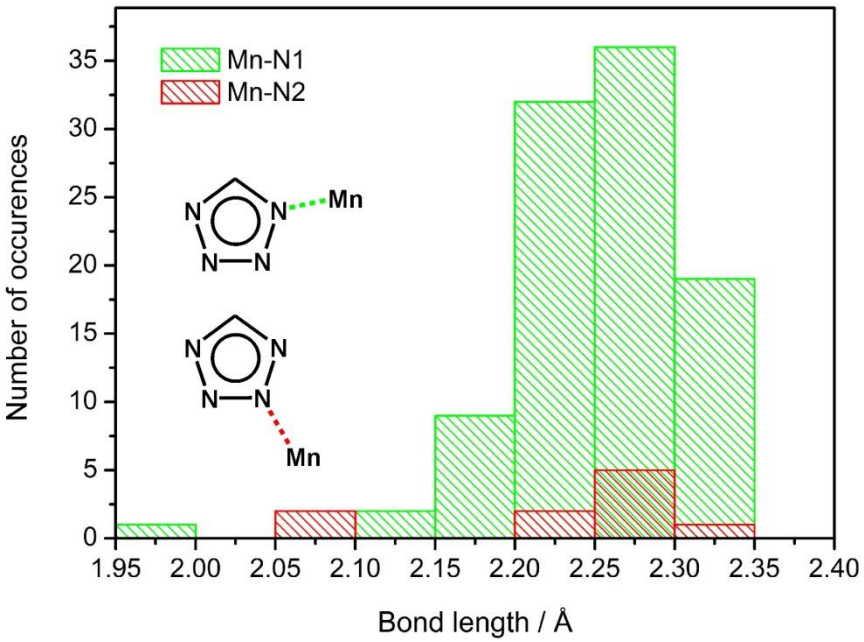

Fig. S9 Mn-N bond statistics for tetrazolate /tetrazole complexes, depicted using separate binning for the two different N-donor atom types. A sampling of 67 structures from 81 available in the CSD (v. 5.33, with updates up to Feb. 2012) with parametrizable N-M bonds length were used. No symmetry adjustment was performed: all bonds, equivalent by symmetry are counted only once).

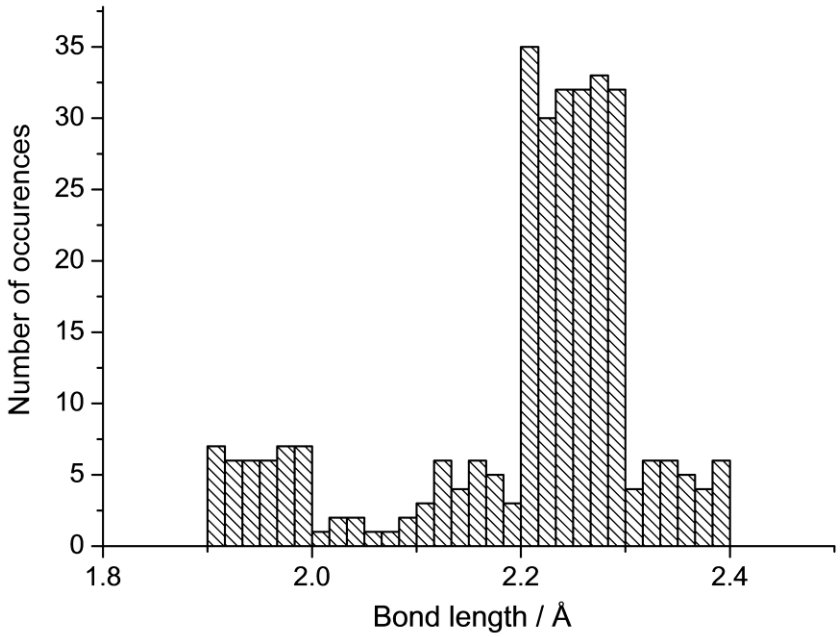

Fig. S10 Mn-N bond statistics for {MnN6} fragment in azole / azolate complexes (the statistics is automatically symmetry adjusted, accounting each bond independently)

Topological analysis of the (4,8)-coordinated alb-4,8-Cmce net

Maximal space-group symmetry: *Cmce* (computed with *Gavrog Systre*) [7]

Unit cell (edges normalized to 1.56): *a* = 2.6938, b = 4.0298; *c* = 4.0257

Coordinates of the nodes:

Vertex	Coordination number	*x*	*y*	*z*	Wyckoff letter	Site symmetry
V1	4	0	0.13829	0.63807	8*f*	*m*
V2	8	0	0	0	4*a*	2/*m*

Coordination sequences (topological density TD_{10}=1510):

Vertex	CS_1	CS_2	CS_3	CS_4	CS_5	CS_6	CS_7	CS_8	CS_9	CS_{10}
V1	4	23	28	95	76	217	148	383	244	601
V2	8	14	56	50	152	110	296	194	488	302

Vertex symbols:

Vertex	Vertex symbol	Point symbol
V1	$4.4.4.4.4.6_8$	$4^5.6$
V2	$4.4.4.4.4.4.4.4.4.4.6_2.6_2.6_2.6_2.6_2.6_2.6_4.6_4.6_4.6_4.6_4.6_4.6_6.6_6.*.*.*.*.*$	$4^{10}.6^{14}.8^4$

Analyses

*Sorption studies on **1***

Sorption isotherms were measured using a Quantachrome iQ automatic gas sorption analyzer equipped with oil-free vacuum pumps (ultimate vacuum $<10^{-8}$ mbar) and valves, which guarantee contamination free measurements.

Approx. 50mg of freshly prepared (prior to evacuation) sample of **1** was soaked in 6 ml of dry methanol for 2 days. The supernatant was removed in inert atmosphere, the sample was pre-dried in 10 Torr vacuum and r.t. and transferred in a nitrogen filled and pre-weighed sample tube capped with a septum; the tube was immediately purged to maintain the strictly inert conditions and weighted. The sample was degassed under vacuum at 70°C for 2h and, for a repeated experiment at 120°C for 12h. The weight of the degassed sample (30.9 mg) was determined by a repeated weighting of the sample tube, which was then transferred to the analysis port of the analyzer. Ultra high purity (UHP, grade 5.0, 99.999%) nitrogen and helium gases were used for the measurements; the latter was used for

performing for the determination of the cold and warm free space. H_2 and N_2 sorption isotherms were measured in liquid nitrogen bath using UHP grade gas sources.

Two nitrogen sorption experiments performed on the activated sample degassed first at 70°C and then at 120°C have demonstrated negligible sorption. Degassing at 120°C caused at least partially loss of crystallinity evidenced by microscopic inspection. Only the hydrogen sorption measurement on the sample degassed at 70°C indicated some adsorption surpassing 0.45 $\%_{wt}$ at 1 bar (Fig. S11) The adsorption and desorption curves have a discontinuity on the first desorption point, which was measured at a 5 time longer equilibration time compared to other points. They disruption evidences slow equilibration and very narrow pores, a fact which is in accordance with negligible nitrogen sorption. The exchange with MeOH proved to be rather slow for efficient activation.

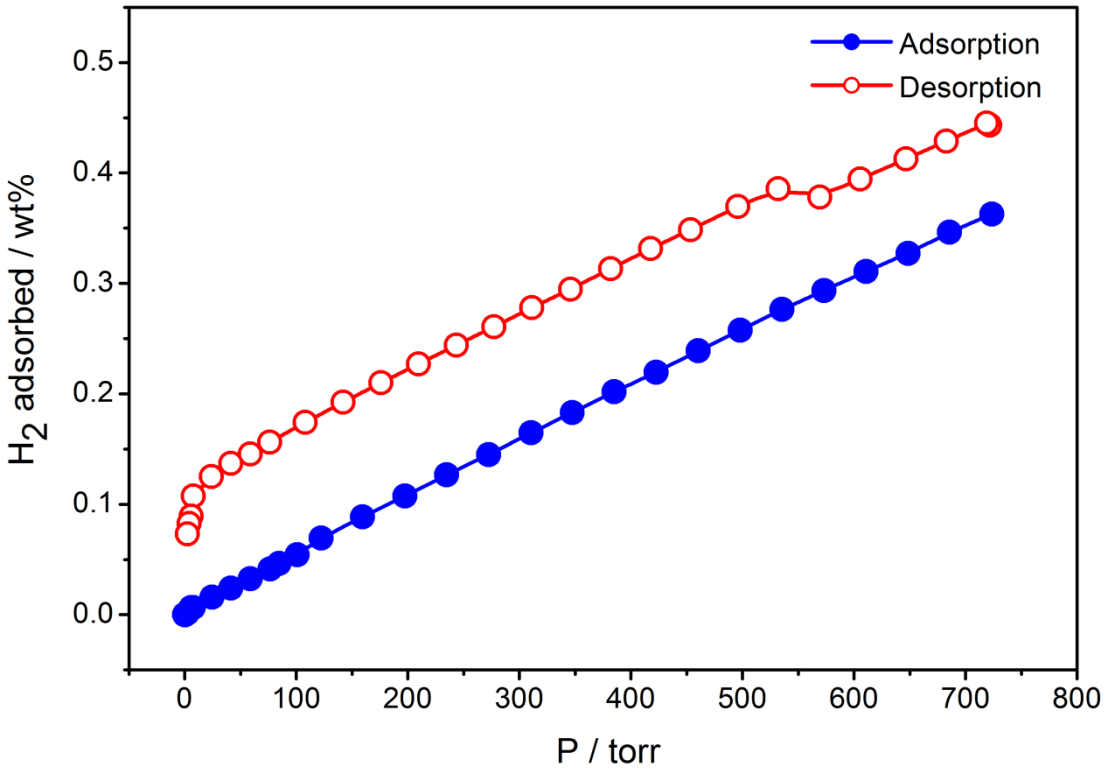

Fig. S11 H_2 sorption isoterms for the activated sample of **1** (please see explanations in the text concerning the disruption of the adsorption and desorption branches)

*TGA of $H_4L1 \cdot 6.5H_2O$, **1** and **2***

$\underline{H_4L^1 \cdot \cdot 6.5H_2O}$

The TGA analysis of the H_4L1 ligand (Fig. SS12) dried on air at room temperature indicated the presence of 3.5 molecules of water per molecule (corresponds to 8.1% weight loss). The obtained value somewhat contradicts with the elemental analysis, which gave 6.5 molecules; the probable reason of discrepancy is the relatively prolonged (30 min) additional drying of the compound in the TGA

measurement chamber. It is clearly visible that a significant part of the water is lost at temperatures below 40°C and a second dehydration stage starts at app. 60°C. Complete dehydration take place at approximately 160C, indicating strong binding of water and presumably fast re-hydration on air, which suggests the air-dried hydrate as the most convenient reagent form with a constant composition.

Approximately at 220°C a second weight loss starts marking the onset of the first phase of the ligand's decomposition, which mostly ends at 300°C. 21.3% loss corresponds to ~12 atoms of nitrogen, suggesting the possible formation of polymeric products based on formal oligomerization of a nitrile group (one residual nitrogen per phenyl group), with triazines among anticipated products. The decomposition is accompanied by a significant exothermic effect.

Slow decomposition continues until 500°C, where a second distinct weight loss occurs, mostly finishing at 600°C. The process could be associated with final carbonization and the loss of the residual nitrogen in a form of volatile carbon containing fragments.

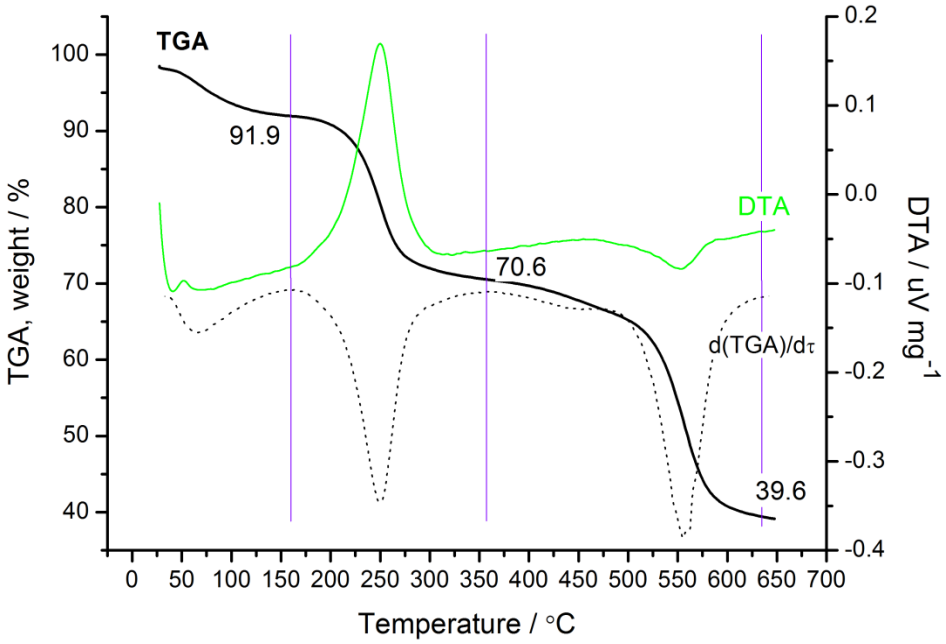

Fig. S12 Thermogravimetric / differential thermal analysis of the hydrated ligand, 1,3,5,7-tetrakis(4-phenyltetrazol-5-yl)adamantane hydrate, $H_4L^1 \cdot 6.5H_2O$

$[Mn_5Cl_2(L^1)_2(H_2O)_4(DMF)_4] \cdot 3\ H_2O \cdot 7\ DMF$, **1**

The weight loss until 100°C comprises 5.4% and could be mostly associated with small amounts of water, remaining after drying in vacuum and diffusing out at elevated temperatures (Fig. SS13). The calculation of water could only be done very approximately as its loss is concomitant with the loss of DMF, which already starts at app. 80°C (Fig. SS13, below), and because of the significant error associated with the small absolute (by weight) water content. The proposed formula unit is a

compromise between TGA and elemental analysis and a formula weight of 2693.2 gives 8.5 molecules of water (5.4% loss), which is probably a slight overestimate. Unfortunately, it was not possible to determinate the relative content of DMF and water according to the MS data at this temperature as the N_2 carrier gas in the TGA instrument had a admixture of air and hence contained water (accordingly, the carrier gas was given as air in the experimental section). The amount of DMF is estimated at 7.5 molecules per formula unit (20.5% weight loss between 94.6°C and 225°C), but it is partially underestimated because of partial overlapping of the DMF caused and the ligand decomposition caused losses. The decomposition of the coordinated ligand proceeds at slightly higher temperatures compared to the non-coordinated one, but the profiles corresponds quite well.

There are two small signals on the DSC curve at app. 60°C (exothermic) and 150°C (endothermic). With a high probability the first corresponds to a structure transformation, which may lead to a structural collapse. As the temperature is low for inducing a direct collapse, especially when the guest molecules are still inside the pores, it is reasonable to suggest a local transformation of the manganese coordination clusters, probably due to their reaction with water.

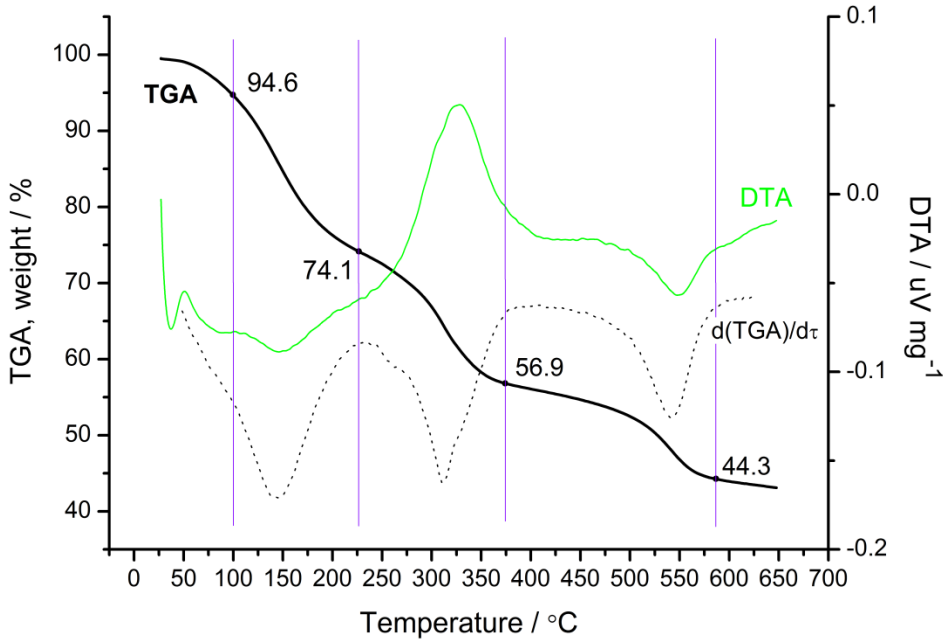

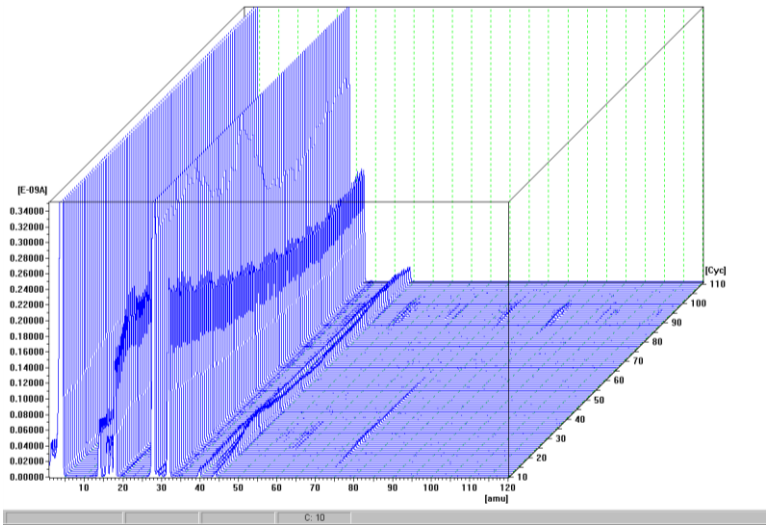

Fig. S13 Thermogravimetric / differential thermal analysis of $[Mn_5Cl_2(L^1)_2(H_2O)_4(DMF)_4] \cdot 3\ H_2O \cdot 7$ DMF, **1** (above). The time dependent mass-spectrum of the exhaust gas. T(°C) = 5.63*(N_{cycles} – 10) + 25, where N_{cycles} corresponds to the number of the cycle; e.g. 20 cycles corresponds to 81.3°C (below)

$[La_2(H_2O)_6(H_5L^2)_2] \cdot$ Solv, **2**

As the sample was not highly pure, no quantitative inferences were made. The TG curve is well defined (Fig. SS14) and consists of three weight loss steps: during the first one, continuing approximately until 110°C, dehydration occurs, while the subsequent weight losses, occurring mainly after 300°C, correspond to the decomposition of the phosphonate ligand.

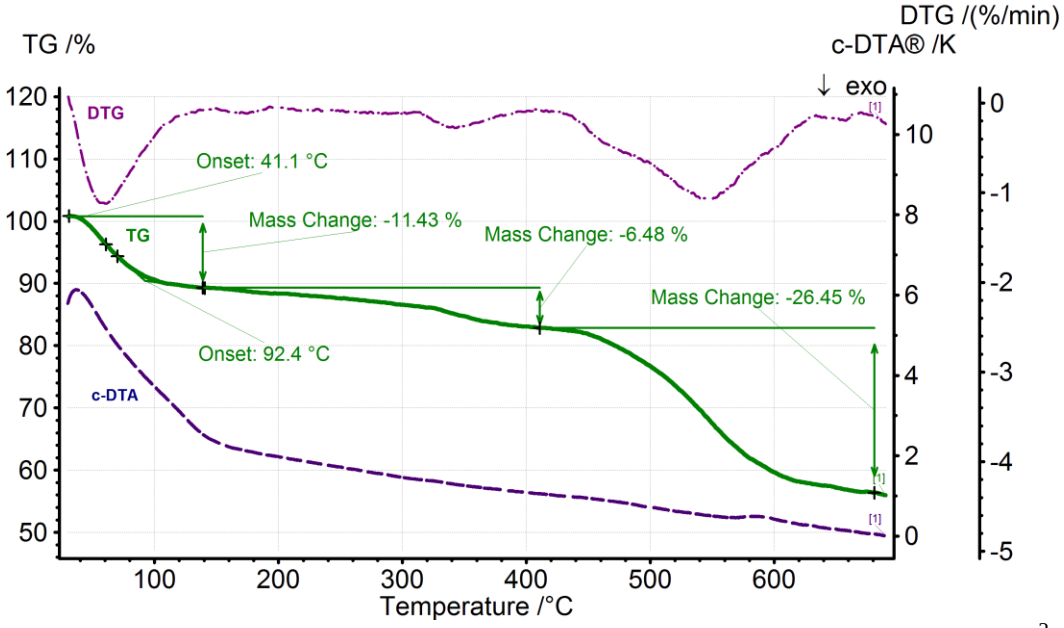

Fig. S14 Thermogravimetric / calculated differential thermal analysis of $[La_2(H_2O)_6(H_5L^2)_2] \cdot$ Solv, **2** (measured on the NETZSCH Tarsus 209 F3)

*IR of $Ad(PhCN)_4$, $H_4L^1 \cdot 6.5H_2O$, **1** and **2***

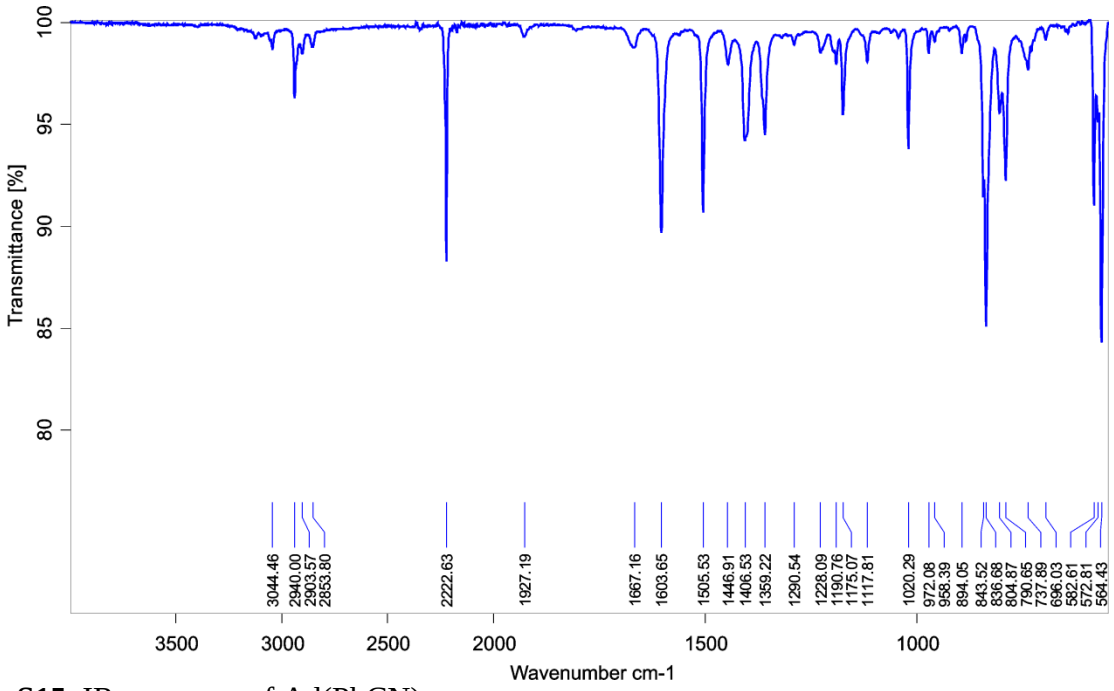

Fig. S15 IR spectrum of $Ad(PhCN)_4$

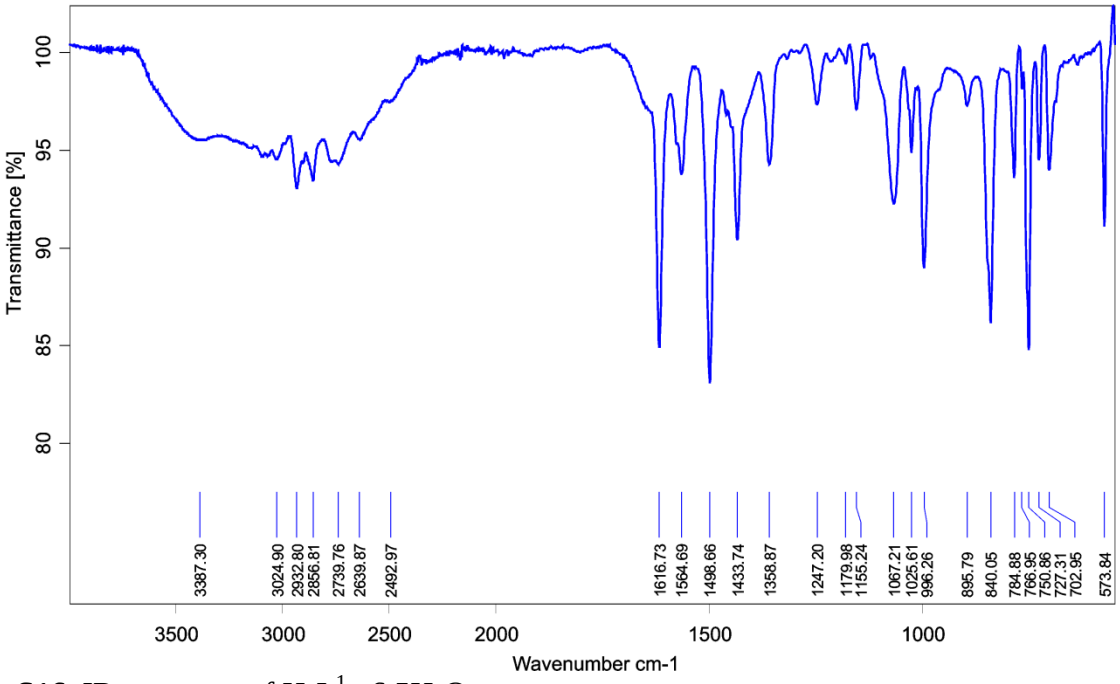

Fig. S16 IR spectrum of $H_4L^1 \cdot 6.5H_2O$

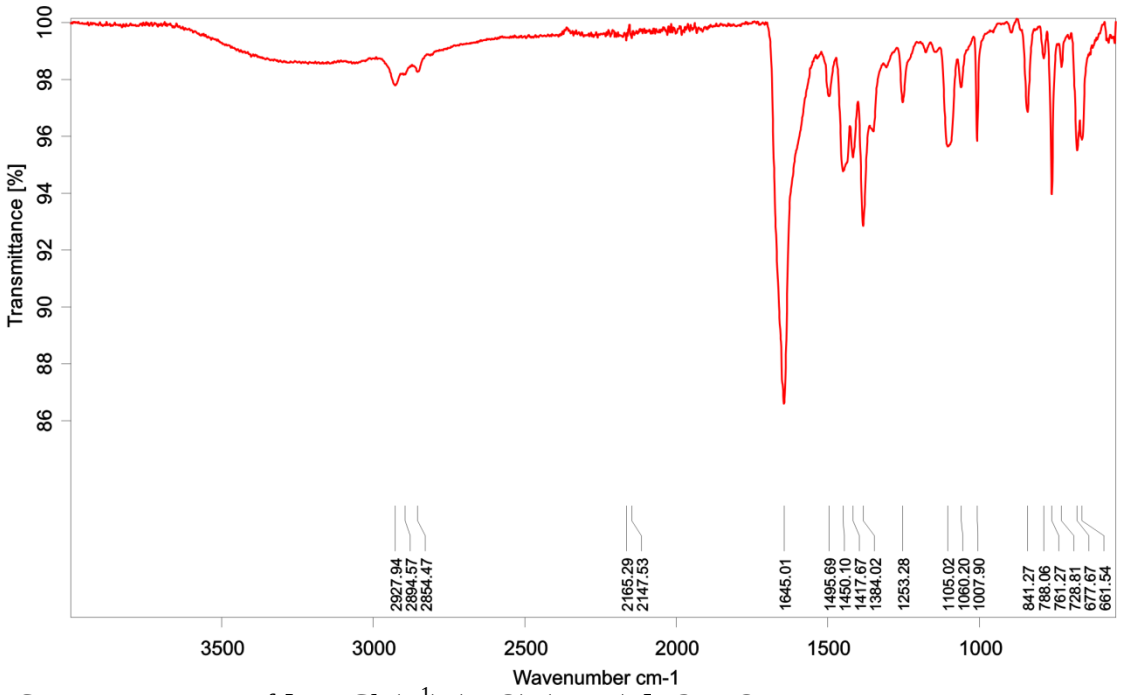

Fig. S17 IR spectrum of $[Mn_5Cl_2(L^1)_2(H_2O)_4(DMF)_4] \cdot 3\ H_2O \cdot 7$ DMF, **1**

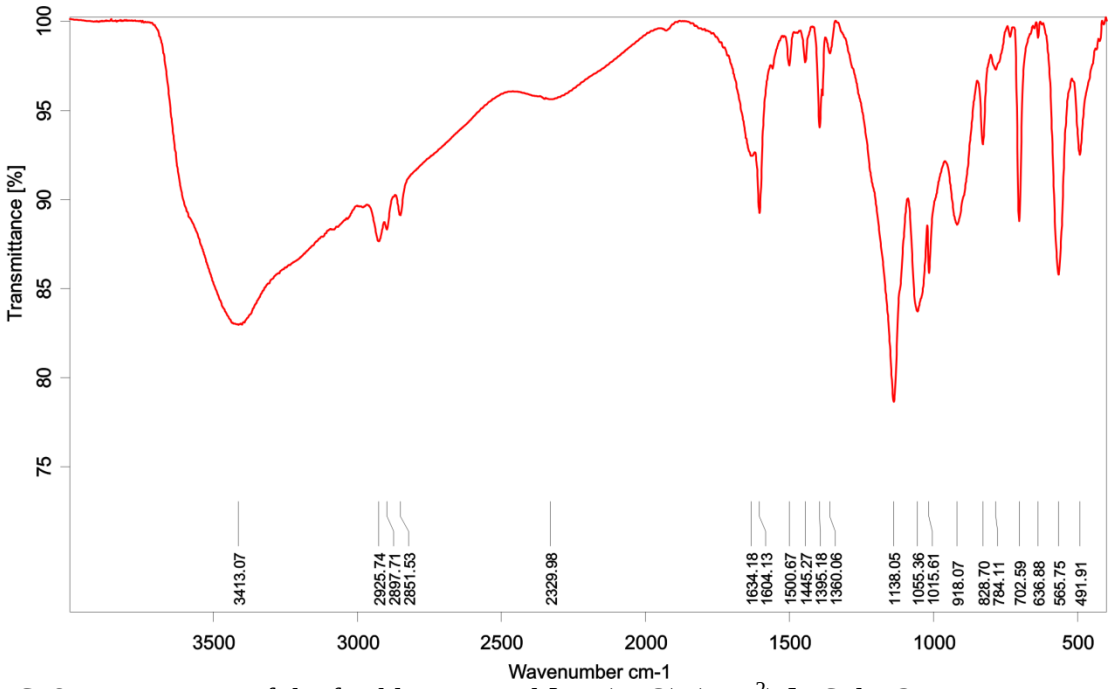

Fig. S18 IR spectrum of the freshly prepared $[La_2(H_2O)_6(H_5L^2)_2] \cdot$ Solv, **2**

*Powder XRD patterns of **1-as** and **2***

The freshly prepared **1-as** after washing with MeOH and drying in inert gas stream demonstrate excellent phase purity and correspondence to the simulated pattern (Fig. SS19). Drying in vacuum (10^{-3} Torr at r.t.), which led to the final product, $[Mn_5Cl_2(L^1)_2(H_2O)_4(DMF)_4] \cdot 3\ H_2O \cdot 7$ DMF, **1**, or prolonged exposure to air (more than a few hours) both caused significant deterioration of crystallinity.

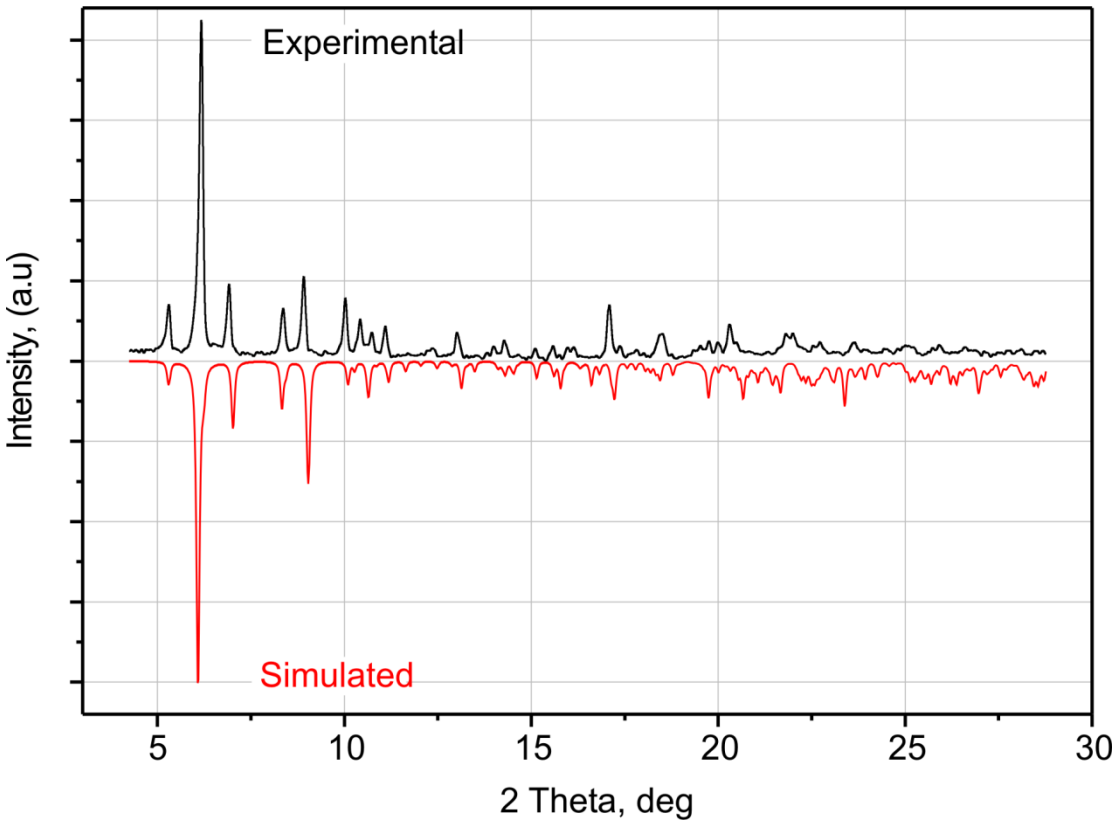

Fig. S19 Comparison of the experimental powder XRD pattern for $[Mn_5Cl_2(L^1)_2(H_2O)_4(DMF)_4] \cdot x\ H_2O \cdot y\ DMF\ z\ H_2O$, **1-as**, with the simulated one, based on the single crystal XRD data.

In contrary, even a short drying of the freshly prepared **2** in inert gas stream causes framework collapse (Fig. SS20). Despite of an unspecified contribution from a second concomitant phase and low quality of the measurement due to scarce amount of the compound available for the analysis (~2 mg) the instability of the structure against loss of solvent is verified.

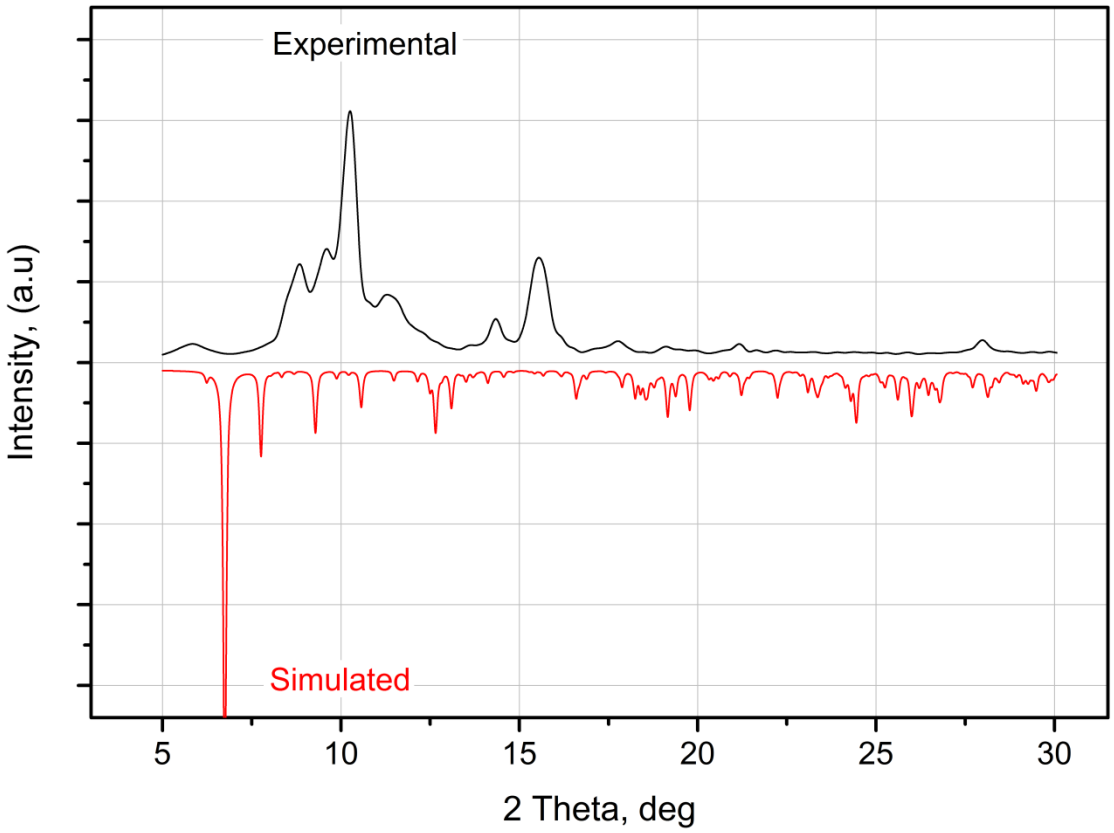

Fig. S20 Comparison of the experimental powder XRD pattern for $[La_2(H_2O)_6(H_5L^2)_2] \cdot Solv$, **2**, with the simulated one, based on the single-crystal X-ray data on **2**.

1 Mercury – Program for Crystal Structure Visualisation, Exploration and Analysis, The Cambridge Crystallographic Data Centre (CCDC). Copyright © (2001-2009).

2 V. R. Reichert and L. J. Mathias, *Macromolecules*, 1994, **27**, 7015.

3 APEX2 2011.3 (Bruker AXS Inc., 2011)

4 SAINT V7.68a (Bruker AXS Inc., 2009)

5 TWINABS V2008/4 (Bruker AXS Inc., 2008)

6 G. M. Sheldrick, *Acta Crystallogr., Sect. A.* **2008**, *64*, 112-122.

7 O. Delgado-Friedrichs, Gavrog: generation, analysis and visualization of reticular ornaments, Web project, 2008 (http://gavrog.sourceforge.net/)